

---

# The Dual Information Bottleneck

---

**Zoe Piran**

Racah Institute of Physics  
The Hebrew University of Jerusalem  
Jerusalem, Israel  
zoe.piran@mail.huji.ac.il

**Ravid Shwartz-Ziv**

School of Computer Science  
The Hebrew University of Jerusalem  
Jerusalem, Israel  
ravid.ziv@mail.huji.ac.il

**Naftali Tishby**

School of Computer Science  
The Hebrew University of Jerusalem  
Jerusalem, Israel  
tishby@cs.huji.ac.il

## Abstract

The Information Bottleneck (IB) framework is a general characterization of optimal representations obtained using a principled approach for balancing accuracy and complexity. Here we present a new framework, the Dual Information Bottleneck (dualIB), which resolves some of the known drawbacks of the IB. We provide a theoretical analysis of the dualIB framework; (i) solving for the structure of its solutions (ii) unraveling its superiority in optimizing the *mean prediction error exponent* and (iii) demonstrating its ability to preserve exponential forms of the original distribution. To approach large scale problems, we present a novel variational formulation of the dualIB for Deep Neural Networks. In experiments on several data-sets, we compare it to a variational form of the IB. This exposes superior Information Plane properties of the dualIB and its potential in improvement of the error.

## 1 Introduction

The Information Bottleneck (IB) method [1], is an information-theoretic framework for describing efficient representations of a “input” random variable  $X$  that preserve the information on an “output” variable  $Y$ . In this setting the joint distribution of  $X$  and  $Y$ ,  $p(x, y)$ , defines the problem, or rule, and the training data are a finite sample from this distribution. The stochastic nature of the label is essential for the analytic regularity of the IB problem. In the case of deterministic labels, we assume a *noise model* which induces a distribution. The representation variable  $\hat{X}$  is in general a stochastic function of  $X$  which forms a Markov chain  $Y \rightarrow X \rightarrow \hat{X}$ , and it depends on  $Y$  only through the input  $X$ . We call the map  $p(\hat{x} | x)$  the *encoder* of the representation and denote by  $p(y | \hat{x})$  the *Bayes optimal decoder* for this representation; i.e., the best possible prediction of the *desired label*  $Y$  from the representation  $\hat{X}$ .

The IB has direct successful applications for representation learning in various domains, from vision and speech processing [2], to neuroscience [3], and Natural Language Processing [4]. Due to the notorious difficulty in estimating mutual information in high dimension, variational approximations to the IB have been suggested and applied also to Deep Neural Networks (DNNs) [e.g., 5, 6, 7]. Additionally, following [8], several recent works tackled the problem of understanding DNNs using the IB principle [9, 10]

Still, there are several drawbacks to the IB framework which motivated this work. While the standard approach in representation learning is to use the topology or a specific parametric model over the input, the IB is completely non-parametric and it operates only on the probability space. In addition, the IB formulation does not relate to the task of prediction over unseen patterns and assumes full access to the joint probability of the patterns and labels.

Here, we resolve the above drawbacks by introducing a novel framework, the Dual Information Bottleneck (dualIB). The dualIB can account for known features of the data and use them to make better predictions over unseen examples, from small samples for large scale problems. Further, it emphasizes the prediction variable,  $\hat{Y}$ , which wasn't present in the original IB formulation.

### 1.1 Contributions of this work

We present here the Dual Information Bottleneck (dualIB) aiming to obtain optimal representations, which resolves the IB drawbacks:

- We provide a theoretical analysis which obtains an analytical solution to the framework and compare its behaviour to the IB.
- For data which can be approximated by exponential families we provide closed form solutions, dualExpIB, which preserves the sufficient statistics of the original distribution.
- We show that by accounting for the prediction variable, the dualIB formulation optimizes a bound over the error exponent.
- We present a novel variational form of the dualIB for Deep Neural Networks (DNNs) allowing its application to real world problems. Using it we empirically investigate the dynamics of the dualIB and validate the theoretical analysis.

## 2 Background

The Information Bottleneck (IB) framework is defined as the trade off between the encoder and decoder mutual information values. It is defined by the minimization of the Lagrangian:

$$\mathcal{F}[p_\beta(\hat{x} | x); p_\beta(y | \hat{x})] = I(X; \hat{X}) - \beta I(Y; \hat{X}), \quad (1)$$

independently over the convex sets of the normalized distributions,  $\{p_\beta(\hat{x} | x)\}$ ,  $\{p_\beta(\hat{x})\}$  and  $\{p_\beta(y | \hat{x})\}$ , given a positive Lagrange multiplier  $\beta$  constraining the information on  $Y$ , while preserving the Markov Chain  $Y \rightarrow X \rightarrow \hat{X}$ . Three self-consistent equations for the optimal encoder-decoder pairs, known as the IB *equations*, define the solutions to the problem. An important characteristic of the equations is the existence of critical points along the optimal line of solutions in the *information plane* (presenting  $I(Y; \hat{X})$  vs.  $I(X; \hat{X})$ ) [11, 12]. The IB optimization trade off can be considered as a generalized rate-distortion problem [13] with the distortion function,  $d_{IB}(x, \hat{x}) = D[p(y | x) || p_\beta(y | \hat{x})]$ . For more background on the IB framework see §A.

## 3 The Dual Information Bottleneck

Supervised learning is generally separated into two phases: the training phase, in which the internal representations are formed from the training data, and the prediction phase, in which these representations are used to predict labels of new input patterns [14]. To explicitly address these different phases we add to the IB Markov chain another variable,  $\hat{Y}$ , the *predicted label* from the trained representation, which obtains the same values as  $Y$  but is distributed differently:

$$Y \xrightarrow{\text{training}} X \rightarrow \hat{X}_\beta \xrightarrow{\text{prediction}} \hat{Y}. \quad (2)$$

The left-hand part of this chain describes the representation training, while the right-hand part is the Maximum Likelihood prediction using these representations [15]. So far the prediction variable  $\hat{Y}$  has not been a part of the IB optimization problem. It has been implicitly assumed that the *Bayes*

optimal decoder,  $p_\beta(y | \hat{x})$ , which maximizes the full representation-label information,  $I(Y; \hat{X})$ , for a given  $\beta$ , is also the best choice for making predictions. Namely, the prediction of the label,  $\hat{Y}$ , from the representation  $\hat{X}_\beta$  through the right-hand Markov chain by the mixture using the internal representations,  $p_\beta(\hat{y} | x) \equiv \sum_{\hat{x}} p_\beta(y = \hat{y} | \hat{x}) p_\beta(\hat{x} | x)$ , is optimal when  $p_\beta(y | \hat{x})$  is the *Bayes optimal decoder*. However, this is not necessarily the case, for example when we train from finite samples [16].

Focusing on the prediction problem, we define the dualIB distortion by switching the order of the arguments in the KL-divergence of the original IB distortion, namely:

$$d_{\text{dualIB}}(x, \hat{x}) = D[p_\beta(y | \hat{x}) || p(y | x)] = \sum_y p_\beta(y | \hat{x}) \log \frac{p_\beta(y | \hat{x})}{p(y | x)}. \quad (3)$$

In geometric terms this is known as the *dual* distortion problem [17]. The dualIB optimization can then be written as the following rate-distortion problem:

$$\mathcal{F}^*[p_\beta(\hat{x} | x); p_\beta(y | \hat{x})] = I(X; \hat{X}) + \beta \mathbb{E}_{p_\beta(x, \hat{x})}[d_{\text{dualIB}}(x, \hat{x})]. \quad (4)$$

As the decoder defines the prediction stage ( $p_\beta(y = \hat{y} | \hat{x})$ ) we can write (see proof in §B) the average distortion in terms of mutual information on  $\hat{Y}$ ,  $I(\hat{X}; \hat{Y})$  and  $I(X; \hat{Y})$ :

$$\mathbb{E}_{p_\beta(x, \hat{x})}[d_{\text{dualIB}}(x, \hat{x})] = \underbrace{I(\hat{X}; \hat{Y}) - I(X; \hat{Y})}_{(a)} + \underbrace{\mathbb{E}_{p(x)}[D[p_\beta(\hat{y} | x) || p(y = \hat{y} | x)]]}_{(b)}. \quad (5)$$

This is similar to the known IB relation:  $\mathbb{E}_{p_\beta(x, \hat{x})}[d_{\text{IB}}(x, \hat{x})] = I(Y; X) - I(Y; \hat{X})$  with an extra positive term (b). Both terms, (a) and (b), vanish precisely when  $\hat{X}$  is a sufficient statistic for  $X$  with respect to  $\hat{Y}$ . In such a case we can reverse the order of  $X$  and  $\hat{X}$  in the Markov chain (2). This replaces the roles of  $Y$  and  $\hat{Y}$  as the variable for which the representations,  $\hat{X}_\beta$ , are approximately minimally sufficient statistics. In that sense the dualIB shifts the emphasis from the training phase to the prediction phase. This implies that minimizing the dualIB functional maximizes a lower bound on the mutual information  $I(X; \hat{Y})$ .

### 3.1 The dualIB equations

Solving the dualIB minimization problem (4), we obtain a set of self consistent equations. Generalized Blahut-Arimoto (BA) iterations between them converges to an optimal solution. The equations are similar to the original IB equations with the following modifications: (i) Replacing the distortion by its dual in the encoder update; (ii) Updating the decoder by the encoder's geometric mean of the data distributions  $p(y | x)$ .

**Theorem 1.** *The dualIB equations are given by:*

$$\begin{cases} (i) & p_\beta(\hat{x} | x) = \frac{p_\beta(\hat{x})}{Z_{\hat{x}|x}(x; \beta)} e^{-\beta D[p_\beta(y|\hat{x}) || p(y|x)]} \\ (ii) & p_\beta(\hat{x}) = \sum_x p_\beta(\hat{x} | x) p(x) \\ (iii) & p_\beta(y | \hat{x}) = \frac{1}{Z_{y|\hat{x}}(\hat{x}; \beta)} \prod_x p(y | x) p_\beta(x|\hat{x}) \end{cases}, \quad (6)$$

where  $Z_{\hat{x}|x}(x; \beta)$ ,  $Z_{y|\hat{x}}(\hat{x}; \beta)$  are normalization terms.

The proof is given in §C. It is evident that the basic structure of the equations of the dualIB and IB is similar and they approach each other for large values of  $\beta$ . In the following sections we explore the implication of the differences on the properties of the new framework.

### 3.2 The critical points of the dualIB

As mentioned in §2 and [11], the “skeleton” of the IB optimal bound (the information curve) is constituted by the critical points in which the topology (cardinality) of the representation changes. Using perturbation analysis over the dualIB optimal representations we find that small changes in the encoder and decoder that satisfy (6) for a given  $\beta$  are approximately determined through a nonlinear eigenvalues problem.<sup>1</sup>

<sup>1</sup>For simplicity we ignore here the possible interactions between the different representations.

**Theorem 2.** *The dualIB critical points are given by non-trivial solutions of the nonlinear eigenvalue problem:*

$$[I - \beta C_{xx'}^{\text{dualIB}}(\hat{x}, \beta)] \delta \log p_\beta(x' | \hat{x}) = 0, \quad [I - \beta C_{yy'}^{\text{dualIB}}(\hat{x}, \beta)] \delta \log p_\beta(y' | \hat{x}) = 0. \quad (7)$$

*The matrices  $C_{xx'}^{\text{dualIB}}(\hat{x}; \beta)$ ,  $C_{yy'}^{\text{dualIB}}(\hat{x}; \beta)$  have the same eigenvalues  $\{\lambda_i\}$ , with  $\lambda_1(\hat{x}) = 0$ . With binary  $y$ , the critical points are obtained at  $\lambda_2(\hat{x}) = \beta^{-1}$ .*

The proof to Theorem 2 along with the structure of the matrices  $C_{xx'}^{\text{dualIB}}(\hat{x}; \beta)$ ,  $C_{yy'}^{\text{dualIB}}(\hat{x}; \beta)$  is given in §D. We found that this solution is similar to the nonlinear eigenvalues problem for the IB, given in §A. As in the IB, at the critical points we observe cusps with an undefined second derivative in the mutual information values as functions of  $\beta$  along the optimal line. That is the general structure of the solutions is preserved between the frameworks, as can be seen in Figure 1c.

The *Information Plane*,  $I_y = I(\hat{X}; Y)$  vs.  $I_x = I(\hat{X}; X)$ , is the standard depiction of the compression-prediction trade-off of the IB and has known analytic properties[18]. First, we note that both curves obey similar constraints, as given in *lemma 3* below.

**Lemma 3.** *along the optimal lines of  $I_x(\beta)$  and  $I_y(\beta)$  the curves are non-decreasing piece-wise concave functions of  $\beta$ . When their second derivative (with respect to  $\beta$ ) is defined, it is strictly negative.*

Next, comparing the dualIB’s and IB’s information planes we find several interesting properties which are summarized in the following Theorem (see §E for the proof).

**Theorem 4.** (i) *The critical points of the two algorithms alternate,  $\forall i, i + 1, \beta_{c,i}^{\text{dualIB}} \leq \beta_{c,i}^{\text{IB}} \leq \beta_{c,i+1}^{\text{dualIB}} \leq \beta_{c,i+1}^{\text{IB}}$ .* (ii) *The distance between the two information curves is minimized at  $\beta_c^{\text{dualIB}}$ .* (iii) *The two curves approach each other as  $\beta \rightarrow \infty$ .*

From Theorem 4 we deduce that as the dimensionality of the problem increases (implying the number of critical points grows) the dualIB’s approximation of the IB’s information plane becomes tighter. We illustrate the behavior of the dualIB’s solutions in comparison to the IB’s on a low-dimensional problem that is easy to analyze and visualize, with a binary  $Y$  and only 5 possible inputs  $X$  (the complete definition is given in §D.1). For any given  $\beta$ , the encoder-decoder iterations converge to stationary solutions of the dualIB or IB *equations*. The evolution of the optimal decoder,  $p_\beta(y = 0 | \hat{x})$ ,  $\forall \hat{x} \in \hat{X}$ , as a function of  $\beta$ , forms a *bifurcation diagram* (Figure 1a), in which the critical points define the location of the bifurcation. At the critical points the number of iterations diverges (Figure 1b). While the overall structure of the solutions is similar, we see a “shift” in the appearance of the representation splits between the two frameworks. Specifically, as predicted by Theorem 4 the dualIB bifurcations occur at lower  $\beta$  values than those of the IB. The inset of Figure 1c depicts this comparison between the two information curves. While we know that  $I_y^{\text{IB}}(\beta)$  is always larger, we see that for this setting the two curves are almost indistinguishable. Looking at  $I_y$  as a function of  $\beta$  (Figure 1c) the importance of the critical points is revealed as the corresponding cusps along these curves correspond to “jumps” in the accessible information. Furthermore, the distance between the curves is minimized precisely at the dual critical points, as predicted by the theory.

## 4 The Exponential Family dualIB

One of the major drawbacks of the IB is that it fails to capture an existing parameterization of the data, that act as minimal sufficient statistics for it. Exponential families are the class of parametric distributions for which minimal sufficient statistics exist, forming an elegant theoretical core of parametric statistics and often emerge as maximum entropy [19] or stochastic equilibrium distributions, subject to observed expectation constraints. As the IB ignores the structure of the distribution, given data from an exponential family it won’t consider these known features. Contrarily, the dualIB accounts for this structure and its solution are given in terms of these features, defining the dualExpIB equations.

We consider the case in which the rule distribution is of the form,  $p(y | x) = e^{-\sum_{r=0}^d \lambda^r(y) A_r(x)}$ , where  $A_r(x)$  are  $d$  functions of the input  $x$  and  $\lambda^r(y)$  are functions of the label  $y$ , or the parameters of this exponential family<sup>2</sup>. For exponential forms the mutual information,  $I(X; Y)$ , is fully captured by

<sup>2</sup> The normalization factors,  $Z_{y|x}(x)$ , are written, for brevity, as  $\lambda_x^0 \equiv \log(\sum_y \prod_{r=1}^d e^{-\lambda^r(y) A_r(x)})$  with  $A_0(x) \equiv 1$ . We do not constrain the marginal  $p(x)$ .

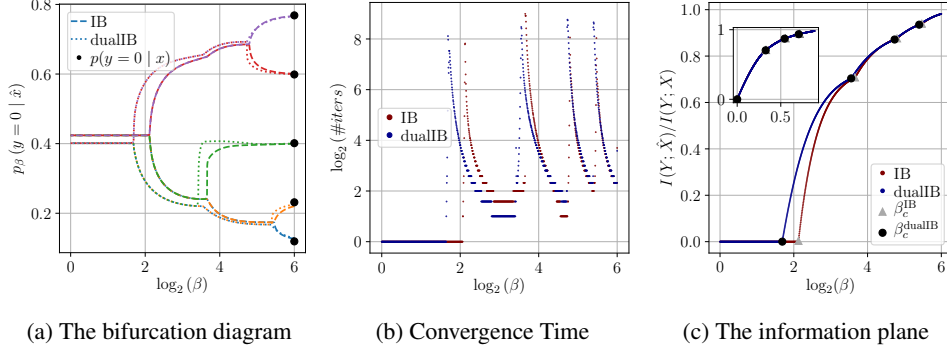


Figure 1: (a) The *bifurcation diagram*; each color corresponds to one component of the representation  $\hat{x} \in \hat{X}$  and depicts the decoder  $p_\beta(y = 0 | \hat{x})$ . Dashed lines represent the IB's solution and dotted present the dualIB's. The black dots denote the input distribution  $p(y = 0 | x)$ . (b) Convergence time the BA algorithms as a function of  $\beta$ . (c) The desired label Information  $I_y^{\text{IB}}(\beta)$  and  $I_y^{\text{dualIB}}(\beta)$  as functions of  $\beta$ . The inset shows the information plane,  $I_y$  vs.  $I_x$ . The black dots are the dualIB's critical points,  $\beta_c^{\text{dualIB}}$ , and the grey triangles are the IB's,  $\beta_c^{\text{IB}}$

the  $d$  conditional expectations. This implies that all the relevant information (in the training sample) is captured by  $d$ -dimensional empirical expectations which can lead to a reduction in computational complexity.

Next we show that for the dualIB, for all values of  $\beta$ , this dimension reduction is preserved or improved along the dual information curve. The complete derivations are given in §F.

**Theorem 5.** (dualExpIB) *For data from an exponential family the optimal encoder-decoder of the dualIB are given by:*

$$\begin{aligned}
 p_\beta(\hat{x} | x) &= \frac{p_\beta(\hat{x}) e^{\beta \lambda_\beta^0(\hat{x})}}{Z_{\hat{x}|x}(x; \beta)} e^{-\beta \sum_{r=1}^d \lambda_\beta^r(\hat{x}) [A_r(x) - A_{r,\beta}(\hat{x})]} \\
 p_\beta(y | \hat{x}) &= e^{-\sum_{r=1}^d \lambda^r(y) A_{r,\beta}(\hat{x}) - \lambda_\beta^0(\hat{x})}, \quad \lambda_\beta^0(\hat{x}) = \log\left(\sum_y e^{-\sum_{r=1}^d \lambda^r(y) A_{r,\beta}(\hat{x})}\right), \quad (8)
 \end{aligned}$$

with the constraints and multipliers expectations,

$$A_{r,\beta}(\hat{x}) \equiv \sum_x p_\beta(x | \hat{x}) A_r(x), \quad \lambda_\beta^r(\hat{x}) \equiv \sum_y p_\beta(y | \hat{x}) \lambda^r(y), \quad 1 \leq r \leq d. \quad (9)$$

This defines a simplified iterative algorithm for solving the dualExpIB problem. Given the mapping of  $x \in X$  to  $\{A_r(x)\}_{r=1}^d$  the problem is completely independent of  $x$  and we can work in the lower dimensional embedding of the features,  $A_r(x)$ . Namely, the update procedure is reduced to the dimensions of the sufficient statistics. Moreover, the representation is given in terms of the original features, a desirable feature for any model based problem.

## 5 Optimizing the error exponent

The dualIB optimizes an upper bound on the error exponent of the representation multi class testing problem. The error exponent accounts for the decay of the prediction error as a function of data size  $n$ . This implies the dualIB tends to minimize the prediction error. For the classical binary hypothesis testing, the classification Bayes error,  $P_e^{(n)}$ , is the weighted sum of type 1 and type 2 errors. For large  $n$ , both errors decay exponentially with the test size  $n$ , and the best error exponent,  $D^*$ , is given by the Chernoff information. The Chernoff information is also a measure of distance defined as,  $C(p_0, p_1) = \min_{0 < \lambda < 1} \{\log \sum_x p_0^\lambda(x) p_1^{1-\lambda}(x)\}$ , and we can understand it as an optimization on the log-partition function of  $p_\lambda$  to obtain  $\lambda$  (for further information see [13] and §G).

The intuition behind the optimization of  $D^*$  by the dualIB is in its distortion, the order of the prediction and the observation which implies the use of geometrical mean. The best achievable exponent (see

[13]) in Bayesian probability of error is given by the KL-distortion between  $p_{\lambda^*}$  ( $\propto p_0^{\lambda^*}(x)p_1^{1-\lambda^*}(x)$ ) to  $p_0$  or  $p_1$ , such that  $p_{\lambda^*}$  is the mid point between  $p_0$  and  $p_1$  on the geodesic of their geometric means. By mapping the dualIB decoder to  $\lambda$ , it follows that the above minimization is proportional to the log-partition function of  $p_\beta(x | \hat{x})$ , namely we obtain the mapping  $p_\beta(x | \hat{x}) = p_\lambda$ .

In the generalization to multi class classification the error exponent is given by the pair of hypotheses with the minimal Chernoff information [20]. However, finding this value is generally difficult as it requires solving for each pair in the given classes. Thus, we consider an upper bound to it, the mean of the Chernoff information terms over classes. The representation variable adds a new dimension on which we average on and we obtain a bound on the optimal (in expectation over  $\hat{x}$ ) achievable exponent,  $\hat{D}_\beta = \min_{p_\beta(y|\hat{x}), p_\beta(\hat{x}|x)} \mathbb{E}_{p_\beta(y,\hat{x})}[D[p_\beta(x | \hat{x}) | p(x | y)]]$ . This expression is bounded from above by the dualIB minimization problem. Thus, the dualIB (on expectation) minimizes the prediction error for every  $n$ . A formal derivation of the above along with an analytical example of a multi class classification problem is given in §G. In §6.1.3 we experimentally demonstrate that this also holds for a variational dualIB framework using a DNN.

## 6 Variational Dual Information Bottleneck

The Variational Information Bottleneck (VIB) approach introduced by Alemi et al. [5] allows to parameterize the IB model using Deep Neural Networks (DNNs). The variational bound of the IB is obtained using DNNs for both the encoder and decoder. Since then, various extensions have been made [21, 22] demonstrating promising attributes. Recently, along this line, the Conditional Entropy Bottleneck (CEB) [23] was proposed. The CEB provides variational optimizing bounds on  $I(Y; \hat{X})$ ,  $I(X; \hat{X})$  using a variational decoder  $q(y | \hat{x})$ , variational conditional marginal,  $q(\hat{x} | y)$ , and a variational encoder,  $p(\hat{x} | x)$ , all implemented by DNNs.

Here, we present the variational dualIB (VdualIB), which optimizes the variational dualIB objective for using in DNNs. Following the CEB formalism, we bound the dualIB objective. We develop a variational form of the dualIB distortion and combine it with the bound for  $I(X; \hat{X})$  (as in the CEB). This gives us the following Theorem (for the proof see §H.1.).

**Theorem 6.** *The VdualIB objective is given by:*

$$\min_{q(\hat{x}|y), p(\hat{x}|x)} \left\{ \mathbb{E}_{\tilde{p}(y|x)p(\hat{x}|x)p(x)} \left[ \log \frac{p(\hat{x} | x)}{q(\hat{x} | y)} \right] + \beta \mathbb{E}_{p(y|\hat{x})p(\hat{x}|x)} \left[ \log \frac{p(y | \hat{x})}{\tilde{p}(y | x)} \right] \right\}, \quad (10)$$

where  $\tilde{p}(y | x)$  is a distribution based on the given labels of the data-set, which we relate to as the noise model. Under the assumption that the noise model captures the distribution of the data the above provides a variational upper bound to the dualIB functional (4).

Due to the nature of its objective the dualIB requires a noise model. We must account for the contribution to the objective arising from  $\tilde{p}(y | x)$  which could be ignored in the VIB case. The noise model can be specified by its assumptions over the data-set. In §6.1.2 we elaborate on possible noise models choices and their implications on the performance. Notice that the introduction of  $\tilde{p}(y | x)$  implies that, unlike most machine learning models, the VdualIB does not optimize directly the error between the predicted and desired labels in the training data. Instead, it does so implicitly with respect to the noisy training examples. This is not unique to the VdualIB, as it is equivalent to training with noisy labels, often done to prevent over-fitting. For example, in [24] the authors show that label noise can improve generalization that results in a reduction in the mutual information between the input and the output.

In practice, similarly to the CEB, for the stochastic encoder,  $p(\hat{x} | x)$ , we use the original architecture, replacing the final softmax layer with a linear dense layer with  $d$  outputs. These outputs are taken as the means of a multivariate Gaussian distribution with unit diagonal covariance. For the variational decoder,  $q(y | \hat{x})$ , any classifier network can be used. We take a linear softmax classifier which takes the encoder as its input. The reverse decoder  $q(\hat{x} | y)$  is implemented by a network which maps a one-hot representation of the labels to the  $d$ -dimensional output interpreted as the mean of the corresponding Gaussian marginal.

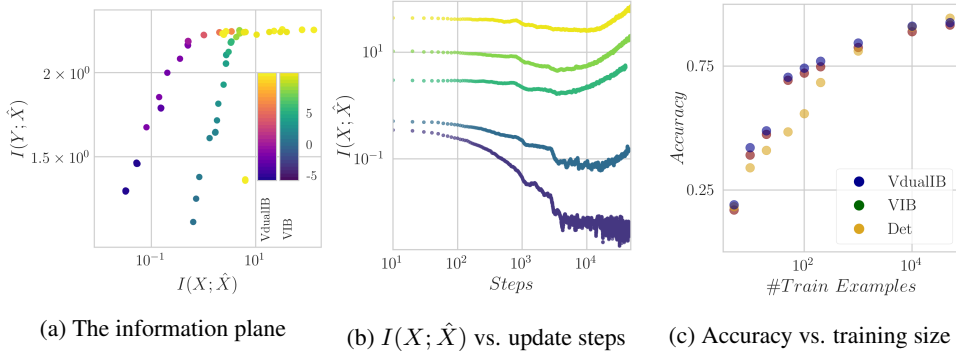


Figure 2: Experiments over FashionMNIST. (a) The information plane of the ConfVdualIB and VIB for a range of  $\beta$  values at the final training step. (b) The evolution of the the ConfVdualIB’s  $I(X; \hat{X})$  along the optimization update steps. (c) The models accuracy as a function of the training set size.

## 6.1 Experiments

To investigate the VdualIB on real-world data we compare it to the CEB model using a DNN over two data-sets, FasionMNIST and CIFAR10. For both, we use a Wide ResNet 28 – 10 [25] as the encoder, a one layer Gaussian decoder and a single layer linear network for the reverse decoder (similarly to the setup in [26]). We use the same architecture to train networks with VdualIB and VIB objectives. (See §H.2 for details on the experimental setup). We note that in our attempts to train over the CIFAR100 data-set the results did not fully agree with the results on the above data-sets (for more information see §H.5). An open source implementation is available here.

### 6.1.1 The variational information plane

As mentioned, the information plane describes the compression-prediction trade-off. It enables us to compare different models and evaluate their “best prediction level” in terms of the desired label information, for each compression level. In [26] the authors provide empirical evidence that information bottlenecking techniques can improve both generalization and robustness. Other works [23, 27, 28] provide both theoretical and conceptual insights into why these improvements occur.

In Figure 2 we present the information plane of the VdualIB where the distribution  $\tilde{p}(y | x)$  (the noise model) is a learnt confusion matrix, ConfVdualIB (similarly to [11]). We compare it to the VIB over a range of  $\beta$  values ( $-5 \leq \log \beta \leq 5$ ). Figure 2a validates that, as expected, the information growth is approximately monotonic with  $\beta$ . Comparing the VdualIB to the VIB model, we can see significant differences between their representations. The VdualIB successfully obtains better compressed representations in comparison to the VIB performance, where only for large values of  $I(X; \hat{X})$  their performances match. As predicted by the theory, in the limit  $\beta \rightarrow \infty$  the models behaviour match. Furthermore, the VdualIB values are smoother and they are spread over the information plane, making it easier to optimize for a specific value in it. In Figure 2b we consider the dynamics of  $I(X; \hat{X})$  for several values of  $\beta$ . Interestingly, at the initial training stage the representation information for all values of  $\beta$  decreases. However, as the training continues, the information increases only for high  $\beta$ s.

### 6.1.2 The VdualIB noise model

As mentioned above, learning with the VdualIB objective requires a choice of a noise model for the distribution  $\tilde{p}(y | \hat{x})$ . To explore the influence of different models on the learning we evaluate four types, with different assumptions on the access to the data. (i) Adding Gaussian noise to the one-hot vector of the true label (GVdualIB); (ii) An analytic Gaussian integration of the log-loss around the one-hot labels; (iii) A pre-computed confusion matrix for the labels (ConfVdualIB) as in [11]; (iv) Using predictions of another trained model as the induced distribution. Where for (i) and (ii) the variance acts as a free parameter determining the noise level. The complexity of the noise models can be characterized by the additional prior knowledge on our data-set they require. While adding Gaussian noise does not require prior knowledge, using a trained model requires access to the prediction for every data sample. The use of a confusion matrix is an intermediate level of prior

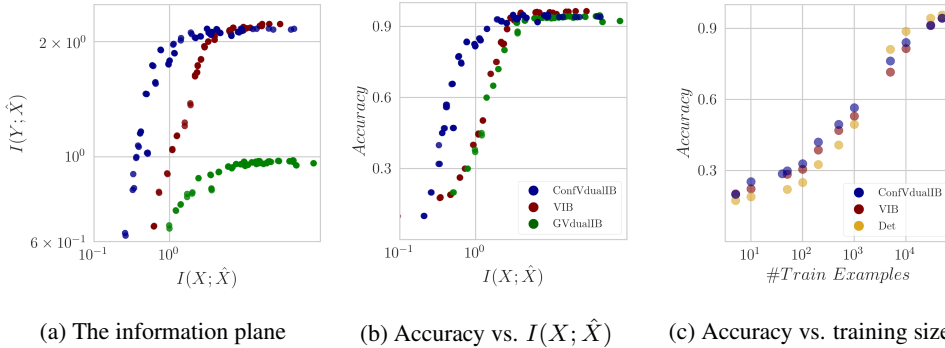


Figure 3: Experiments over CIFAR10. (a) The information plane of the VIB, ConfVdualIB, GVdualIB and VIB for a range of  $\beta$  values. (b) The accuracy of the models as a function of the mutual information,  $I(X; \hat{X})$ . (c) The accuracy of the models as a function of the training set size.

knowledge requiring access only to the  $|\mathcal{Y}| \times |\mathcal{Y}|$  pre-computed matrix. Here we present cases (i) and (iii) (see §H.4 for (ii) and (iv)). Note that although using the VIB does not require the use of a noise model we incorporate it by replacing the labels with  $\hat{p}(y | x)$ . In the analysis below, the results are presented with the VIB trained with the same noise model as the VdualIB (see §H.4 for a comparison between training VdualIB with noise and VIB without it).

Figure 3 depicts the information plane of the CIFAR10 data-set. Figure 3a shows the information obtained from a range of  $\beta$ . The colors depict the different models ConfVdualIB, GVdualIB and the VIB. As we can see, training a VdualIB with Gaussian noise achieves much less information with the labels at any given  $I(X; \hat{X})$ . We note that we verified that this behaviour is consistent over a wide range of variances. The ConfVdualIB model performance is similar to the VIB’s with the former showcasing more compressed representations. When we present the prediction accuracy (Figure 3b), here all models attain roughly the same accuracy values. The discrepancy between the accuracy and information,  $I(Y; \hat{X})$ , is similar to the one discussed in [29].

### 6.1.3 Performance with different training set sizes

Our theoretical analysis (§5) shows that under given assumptions the dualIB bounds the optimal achievable error exponent on expectation hence it optimizes the error for a given data size  $n$ . We turn to test this in the VdualIB setting. We train the models on a subset of the training set and evaluate them on the test set. We compare the VIB and the VdualIB to a deterministic network (Det; Wide Res Net 28-10). Both the VIB and VdualIB are trained over a wide range of  $\beta$  values ( $-5 \leq \log \beta \leq 6$ ). Presented is the best accuracy value for each model at a given  $n$ . Figure 2c and Figure 3c show the accuracy of the models as a function of the training set size over FashionMNIST and CIFAR10 respectively. The VdualIB performance is slightly better in comparison to the VIB, while the accuracy of the deterministic network is lower for small training sets. The superiority of the variational models over the deterministic network is not surprising as minimizing  $I(X; \hat{X})$  acts as regularization.

## 7 Conclusions

We present here the Dual Information Bottleneck (dualIB), a framework resolving some of the known drawbacks of the IB obtained by a mere switch between the terms in the distortion function. We provide the dualIB self-consistent equations allowing us to obtain analytical solutions. A local stability analysis revealed the underlying structure of the critical points of the solutions, resulting in a full bifurcation diagram of the optimal pattern representations. The study of the dualIB objective reveals several interesting properties. First, when the data can be modeled in a parametric form the dualIB preserves this structure and it obtains the representation in terms of the original parameters, as given by the dualExpIB equations. Second, it optimizes the mean prediction error exponent thus improving the accuracy of the predictions as a function of the data size. In addition to the dualIB analytic solutions, we provide a variational dualIB (VdualIB) framework, which optimizes the functional using DNNs. This framework enables practical implementation of the dualIB to real



world data-sets. While a broader analysis is required, the VdualIB experiments shown validate the theoretical predictions. Our results demonstrate the potential advantages and unique properties of the framework.

## References

- [1] Naftali Tishby, Fernando C. Pereira, and William Bialek. The information bottleneck method. In *Proc. of the 37-th Annual Allerton Conference on Communication, Control and Computing*, pages 368–377, 1999.
- [2] Shuang Ma, Daniel McDuff, and Yale Song. Unpaired image-to-speech synthesis with multimodal information bottleneck. In *Proceedings of the IEEE International Conference on Computer Vision*, pages 7598–7607, 2019.
- [3] Elad Schneidman, Noam Slonim, Naftali Tishby, R deRuyter van Steveninck, and William Bialek. Analyzing neural codes using the information bottleneck method. *Advances in Neural Information Processing Systems, NIPS*, 2001.
- [4] Xiang Lisa Li and Jason Eisner. Specializing word embeddings (for parsing) by information bottleneck. In *Proceedings of the 2019 Conference on Empirical Methods in Natural Language Processing and 9th International Joint Conference on Natural Language Processing*, pages 2744–2754, Hong Kong, November 2019. Best Paper Award.
- [5] Alexander A. Alemi, Ian Fischer, Joshua V. Dillon, and Kevin Murphy. Deep variational information bottleneck. *ArXiv*, abs/1612.00410, 2016.
- [6] Sonali Parbhoo, Mario Wieser, and Volker Roth. Causal deep information bottleneck. *ArXiv*, abs/1807.02326, 2018.
- [7] Ben Poole, Sherjil Ozair, Aaron van den Oord, Alexander A Alemi, and George Tucker. On variational bounds of mutual information. *arXiv preprint arXiv:1905.06922*, 2019.
- [8] Ravid Shwartz-Ziv and Naftali Tishby. Opening the Black Box of Deep Neural Networks via Information. *arXiv e-prints*, page arXiv:1703.00810, Mar 2017.
- [9] Charlie Nash, Nate Kushman, and Christopher KI Williams. Inverting supervised representations with autoregressive neural density models. *arXiv preprint arXiv:1806.00400*, 2018.
- [10] Ziv Goldfeld, Ewout van den Berg, Kristjan Greenewald, Igor Melnyk, Nam Nguyen, Brian Kingsbury, and Yury Polyanskiy. Estimating information flow in deep neural networks. *arXiv preprint arXiv:1810.05728*, 2018.
- [11] Tailin Wu and Ian Fischer. Phase transitions for the information bottleneck in representation learning. *arXiv preprint arXiv:2001.01878*, 2020.
- [12] Albert E. Parker, Tomáš Gedeon, and Alexander G. Dimitrov. Annealing and the rate distortion problem. In S. Becker, S. Thrun, and K. Obermayer, editors, *Advances in Neural Information Processing Systems 15*, pages 993–976. MIT Press, 2003.
- [13] Thomas M. Cover and Joy A. Thomas. *Elements of Information Theory (Wiley Series in Telecommunications and Signal Processing)*. Wiley-Interscience, New York, NY, USA, 2006.
- [14] Shai Shalev-Shwartz and Shai Ben-David. *Understanding machine learning: From theory to algorithms*. Cambridge university press, 2014.
- [15] Noam Slonim, Nir Friedman, and Naftali Tishby. Multivariate information bottleneck. *Neural Computation*, 18(8):1739–1789, 2006. PMID: 16771652.
- [16] Ohad Shamir, Sivan Sabato, and Naftali Tishby. Learning and generalization with the information bottleneck. *Theor. Comput. Sci.*, 411:2696–2711, 2010.
- [17] Domenico Felice and Nihat Ay. Divergence functions in information geometry. In Frank Nielsen and Frédéric Barbaresco, editors, *Geometric Science of Information - 4th International Conference, GSI 2019, Toulouse, France, August 27-29, 2019, Proceedings*, volume 11712 of *Lecture Notes in Computer Science*, pages 433–442. Springer, 2019.
- [18] Ran Gilad-bachrach, Amir Navot, and Naftali Tishby. An information theoretic tradeoff between complexity and accuracy. In *In Proceedings of the COLT*, pages 595–609. Springer, 2003.
- [19] E. T. Jaynes. Information theory and statistical mechanics. *Phys. Rev.*, 106:620–630, May 1957.

- [20] M Brandon Westover. Asymptotic geometry of multiple hypothesis testing. *IEEE transactions on information theory*, 54(7):3327–3329, 2008.
- [21] DJ Strouse and David J Schwab. The deterministic information bottleneck. *Neural computation*, 29(6):1611–1630, 2017.
- [22] Adar Elad, Doron Haviv, Yochai Blau, and Tomer Michaeli. Direct validation of the information bottleneck principle for deep nets. In *Proceedings of the IEEE International Conference on Computer Vision Workshops*, pages 0–0, 2019.
- [23] Ian Fischer. The conditional entropy bottleneck. In *URL openreview. net/forum*, 2018.
- [24] Rafael Müller, Simon Kornblith, and Geoffrey E Hinton. When does label smoothing help? In *Advances in Neural Information Processing Systems*, pages 4696–4705, 2019.
- [25] Sergey Zagoruyko and Nikos Komodakis. Wide residual networks. *arXiv preprint arXiv:1605.07146*, 2016.
- [26] Ian Fischer and Alexander A Alemi. Ceb improves model robustness. *arXiv preprint arXiv:2002.05380*, 2020.
- [27] Alessandro Achille and Stefano Soatto. Emergence of invariance and disentanglement in deep representations. *The Journal of Machine Learning Research*, 19(1):1947–1980, 2018.
- [28] Alessandro Achille and Stefano Soatto. Information dropout: Learning optimal representations through noisy computation. *IEEE transactions on pattern analysis and machine intelligence*, 40(12):2897–2905, 2018.
- [29] Michael W Dusenberry, Ghassen Jerfel, Yeming Wen, Yi-an Ma, Jasper Snoek, Katherine Heller, Balaji Lakshminarayanan, and Dustin Tran. Efficient and scalable bayesian neural nets with rank-1 factors. *arXiv preprint arXiv:2005.07186*, 2020.
- [30] Lawrence D. Brown. Fundamentals of statistical exponential families with applications in statistical decision theory. *Lecture Notes-Monograph Series*, 9:i–279, 1986.
- [31] Amichai Painsky and Gregory W. Wornell. Bregman Divergence Bounds and the Universality of the Logarithmic Loss. *arXiv e-prints*, page arXiv:1810.07014, Oct 2018.
- [32] G. Tusnady and I. Csiszar. Information geometry and alternating minimization procedures. *Statistics & Decisions: Supplement Issues*, 1:205–237, 1984.
- [33] Noga Zaslavsky and Naftali Tishby. Deterministic annealing and the evolution of optimal information bottleneck representations. *Preprint*, 2019.
- [34] Jorge R Tredicce, Gian Luca Lippi, Paul Mandel, Basile Charasse, Aude Chevalier, and B Picqué. Critical slowing down at a bifurcation. *American Journal of Physics*, 72(6):799–809, 2004.
- [35] Diederik P Kingma and Jimmy Ba. Adam: A method for stochastic optimization. *arXiv preprint arXiv:1412.6980*, 2014.

## Appendix

### A The Information Bottleneck method

The Information Bottleneck (IB) trade off between the encoder and decoder mutual information values is defined by the minimization of the Lagrangian:

$$\mathcal{F}[p_\beta(\hat{x} | x); p_\beta(y | \hat{x})] = I(X; \hat{X}) - \beta I(Y; \hat{X}), \quad (11)$$

independently over the convex sets of the normalized distributions,  $\{p_\beta(\hat{x} | x)\}$ ,  $\{p_\beta(\hat{x})\}$  and  $\{p_\beta(y | \hat{x})\}$ , given a positive Lagrange multiplier  $\beta$ . As shown in [1, 16], this is a natural generalization of the classical concept of *Minimal Sufficient Statistics* [13], where the estimated parameter is replaced by the output variable  $Y$  and *exact* statistical sufficiency is characterized by the mutual information equality:  $I(\hat{X}; Y) = I(X; Y)$ . The minimality of the statistics is captured by the minimization of  $I(X; \hat{X})$ , due to the Data Processing Inequality (DPI). However, non-trivial minimal sufficient statistics only exist for very special parametric distributions known as exponential families [30]. Thus in general, the IB relaxes the minimal sufficiency problem to a continuous family of representations  $\hat{X}$  which are characterized by the trade off between compression,  $I(X; \hat{X}) \equiv I_X$ , and accuracy,  $I(Y; \hat{X}) \equiv I_Y$ , along a convex line in the *Information-Plane* ( $I_Y$  vs.  $I_X$ ). When the rule  $p(x, y)$  is strictly stochastic, the convex optimal line is smooth and each point along the line is uniquely characterized by the value of  $\beta$ . We can then consider the optimal representations  $\hat{x} = \hat{x}(\beta)$  as encoder-decoder pairs:  $(p_\beta(x | \hat{x}), p_\beta(y | \hat{x}))^3$  - a point in the continuous manifold defined by the Cartesian product of these distribution simplexes. We also consider a small variation of these representations,  $\delta\hat{x}$ , as an infinitesimal change in this (encoder-decoder) continuous manifold (not necessarily on the optimal line(s)).

#### A.1 IB and Rate-Distortion Theory

The IB optimization trade off can be considered as a generalized rate-distortion problem [13] with the distortion function between a data point,  $x$  and a representation point  $\hat{x}$  taken as the KL-divergence between their predictions of the desired label  $y$ :

$$\begin{aligned} d_{\text{IB}}(x, \hat{x}) &= D[p(y | x) || p_\beta(y | \hat{x})] \\ &= \sum_y p(y | x) \log \frac{p(y | x)}{p_\beta(y | \hat{x})}. \end{aligned} \quad (12)$$

The expected distortion  $\mathbb{E}_{p_\beta(x, \hat{x})}[d_{\text{IB}}(x, \hat{x})]$  for the optimal decoder is simply the label-information loss:  $I(X; Y) - I(\hat{X}; Y)$ , using the Markov chain condition. Thus minimizing the expected IB distortion is equivalent to maximizing  $I(\hat{X}; Y)$ , or minimizing (1). Minimizing this distortion is equivalent to minimizing the cross-entropy loss, and it provides an upper-bound to other loss functions such as the  $\mathcal{L}_1$ -loss (due to the Pinsker inequality, see also [31]). Pinsker implies that both orders of the cross-entropy act as an upper bound to the  $\mathcal{L}_1$ -loss,  $\min\{D[q||p], D[p||q]\} \geq \frac{1}{2 \log 2} \|p - q\|_1^2$ .

#### A.2 The IB Equations

For discrete  $X$  and  $Y$ , a necessary condition for the IB (local) minimization is given by the three self-consistent equations for the optimal encoder-decoder pairs, known as the *IB equations*:

$$\begin{cases} (i) & p_\beta(\hat{x} | x) = \frac{p_\beta(\hat{x})}{Z(x; \beta)} e^{-\beta D[p(y|x) || p_\beta(y|\hat{x})]} \\ (ii) & p_\beta(\hat{x}) = \sum_x p_\beta(\hat{x} | x) p(x) \\ (iii) & p_\beta(y | \hat{x}) = \sum_x p(y | x) p_\beta(x | \hat{x}) \end{cases}, \quad (13)$$

where  $Z(x; \beta)$  is the normalization function. Iterating these equations is a generalized, Blahut-Arimoto, alternating projection algorithm [32, 13] and it converges to a stationary point of the Lagrangian, (1) [1]. Notice that the minimizing decoder, ((13)-(iii)), is precisely the *Bayes optimal decoder* for the representation  $\hat{x}(\beta)$ , given the Markov chain conditions.

<sup>3</sup>Here we use the *inverse encoder*, which is in the fixed dimension simplex of distributions over  $X$ .

### A.3 Critical points and critical slowing down

One of the most interesting aspects of the IB equations is the existence of critical points along the optimal line of solutions in the information plane (i.e. the information curve). At these points the representations change topology and cardinality (number of clusters) [33, 12] and they form the skeleton of the information curve and representation space. To identify such points we perform a perturbation analysis of the IB equations:<sup>4</sup>:

$$\delta \log p_\beta(x | \hat{x}) = \beta \sum_y p(y | x) \delta \log p_\beta(y | \hat{x}), \quad (14)$$

$$\delta \log p_\beta(y | \hat{x}) = \frac{1}{p_\beta(y | \hat{x})} \sum_x p(y | x) p_\beta(x | \hat{x}) \delta \log p_\beta(x | \hat{x}). \quad (15)$$

Substituting (15) into (14) and vice versa one obtains:

$$\begin{aligned} \delta \log p_\beta(x | \hat{x}) &= \beta \sum_{y, x'} p(y | x') \frac{p(y | x)}{p_\beta(y | \hat{x})} p_\beta(x' | \hat{x}) \delta \log p_\beta(x' | \hat{x}) \\ \delta \log p_\beta(y | \hat{x}) &= \beta \sum_{x, y'} p(y | x) \frac{p_\beta(x | \hat{x})}{p_\beta(y | \hat{x})} p(y' | x) \delta \log p_\beta(y' | \hat{x}) \end{aligned}$$

Thus by defining the matrices:

$$C_{xx'}^{\text{IB}}(\hat{x}, \beta) = \sum_y p(y | x) \frac{p_\beta(x' | \hat{x})}{p_\beta(y | \hat{x})} p(y | x'), \quad C_{yy'}^{\text{IB}}(\hat{x}, \beta) = \sum_x p(y | x) \frac{p_\beta(x | \hat{x})}{p_\beta(y | \hat{x})} p(y' | x). \quad (16)$$

We obtain the following nonlinear eigenvalues problem:

$$[I - \beta C_{xx'}^{\text{IB}}(\hat{x}, \beta)] \delta \log p_\beta(x' | \hat{x}) = 0, \quad [I - \beta C_{yy'}^{\text{IB}}(\hat{x}, \beta)] \delta \log p_\beta(y' | \hat{x}) = 0, \quad (17)$$

These two matrices have the same eigenvalues and have non-trivial eigenvectors (i.e., different co-existing optimal representations) at the critical values of  $\beta$ , the bifurcation points of the IB solution. At these points the cardinality of the representation  $\hat{X}$  (the number of ‘‘IB-clusters’’) changes due to splits of clusters, resulting in topological phase transitions in the encoder. These critical points form the ‘‘skeleton’’ of the topology of the optimal representations. Between critical points the optimal representations change continuously (with  $\beta$ ). The important computational consequence of critical points is known as *critical slowing down* [34]. For binary  $y$ , near a critical point the convergence time,  $\tau_\beta$ , of the iterations of (13) scales like:  $\tau_\beta \sim 1/(1 - \beta\lambda_2)$ , where  $\lambda_2$  is the second eigenvalue of either  $C_{yy'}^{\text{IB}}$  or  $C_{xx'}^{\text{IB}}$ . At criticality,  $\lambda_2(\hat{x}) = \beta^{-1}$  and the number of iterations diverges. This phenomenon dominates any local minimization of (13) which is based on alternate encoder-decoder optimization.

The appearance of the critical points and the critical slowing-down is visualized in Figure 1 in the main text.

## B The dualIB mathematical formulation

The dualIB is solved with respect to the full Markov chain ( $Y \rightarrow X \rightarrow \hat{X}_\beta \rightarrow \hat{Y}$ ) in which we introduce the new variable,  $\hat{y}$ , the *predicted label*. Thus, in analogy to the IB we want to write the optimization problem in term of  $\hat{Y}$ .

<sup>4</sup>We ignore here the possible interaction between the different representations, for simplicity.

Developing the expected distortion we find:

$$\begin{aligned}
\mathbb{E}_{p_\beta(x, \hat{x})}[d_{\text{dualIB}}(x, \hat{x})] &= \sum_{x, \hat{x}} p_\beta(x, \hat{x}) \sum_{\hat{y}} p_\beta(y = \hat{y} | \hat{x}) \log \frac{p_\beta(y = \hat{y} | \hat{x})}{p(y = \hat{y} | x)} \\
&= \sum_{\hat{x}, \hat{y}} p_\beta(\hat{x}) p_\beta(\hat{y} | \hat{x}) \log \frac{p_\beta(\hat{y} | \hat{x})}{p_\beta(\hat{y})} - \sum_{x, \hat{y}} p(x) p_\beta(\hat{y} | x) \log \frac{p_\beta(\hat{y} | x)}{p_\beta(\hat{y})} \\
&\quad + \sum_{x, \hat{y}} p(x) p_\beta(\hat{y} | x) \log \frac{p_\beta(\hat{y} | x)}{p(y = \hat{y} | x)} \\
&= I(\hat{X}; \hat{Y}) - I(X; \hat{Y}) + \mathbb{E}_{p(x)}[D[p_\beta(\hat{y} | x) \| p(y = \hat{y} | x)]].
\end{aligned}$$

Allowing the dual optimization problem to be written as:

$$\mathcal{F}^*[p(\hat{x} | x); p(y | \hat{x})] = I(X; \hat{X}) - \beta \left\{ I(X; \hat{Y}) - I(\hat{X}; \hat{Y}) - \mathbb{E}_{p(x)}[D[p_\beta(\hat{y} | x) \| p(y = \hat{y} | x)]] \right\}.$$

## C The DualIB solutions

To prove *theorem 2* we want to obtain the normalized distributions minimizing the dualIB rate-distortion problem.

*Proof.* (i) Given that the problem is formulated as a rate-distortion problem the encoder's update rule must be the known minimizer of the distortion function. [13]. Thus the IB encoder with the dual distortion is plugged in. (ii) For the decoder, by considering a small perturbation in the distortion  $d_{\text{dualIB}}(x, \hat{x})$ , with  $\alpha(\hat{x})$  the normalization Lagrange multiplier, we obtain:

$$\begin{aligned}
\delta d_{\text{dualIB}}(x, \hat{x}) &= \delta \left( \sum_y p_\beta(y | \hat{x}) \log \frac{p_\beta(y | \hat{x})}{p(y | x)} + \alpha(\hat{x}) \left( \sum_y p_\beta(y | \hat{x}) - 1 \right) \right) \\
\frac{\delta d_{\text{dualIB}}(x, \hat{x})}{\delta p_\beta(y | \hat{x})} &= \log \frac{p_\beta(y | \hat{x})}{p(y | x)} + 1 + \alpha(\hat{x}).
\end{aligned}$$

Hence, minimizing the expected distortion becomes:

$$\begin{aligned}
0 &= \sum_x p_\beta(x | \hat{x}) \left[ \log \frac{p_\beta(y | \hat{x})}{p(y | x)} + 1 \right] + \alpha(\hat{x}) \\
&= \log p_\beta(y | \hat{x}) - \sum_x p_\beta(x | \hat{x}) \log p(y | x) + 1 + \alpha(\hat{x}),
\end{aligned}$$

which yields Algorithm 1, row 6.  $\square$

Considering the dualIB encoder-decoder, Algorithm 1, we find that  $\mathbb{E}_{p_\beta(x, \hat{x})}[d_{\text{dualIB}}(x, \hat{x})]$  reduces to the expectation of the decoder's log partition function:

$$\begin{aligned}
\mathbb{E}_{p_\beta(x, \hat{x})}[d_{\text{dualIB}}(x, \hat{x})] &= \sum_{x, \hat{x}} p_\beta(x, \hat{x}) \sum_y p_\beta(y | \hat{x}) \log \frac{p_\beta(y | \hat{x})}{p(y | x)} \\
&= -\mathbb{E}_{p_\beta(\hat{x})}[\log Z_{\mathbf{y}|\hat{\mathbf{x}}}(\hat{\mathbf{x}}; \beta)] + \sum_{\hat{x}, y} p_\beta(\hat{x}) \left[ \sum_{x'} p_\beta(x' | \hat{x}) \log p(y | x') - \sum_x p_\beta(x | \hat{x}) \log p(y | x) \right] \\
&= -\mathbb{E}_{p_\beta(\hat{x})}[\log Z_{\mathbf{y}|\hat{\mathbf{x}}}(\hat{\mathbf{x}}; \beta)].
\end{aligned}$$

## D Stability analysis

Here we provide the detailed stability analysis allowing the definition of the matrices  $C_{xx'}^{\text{dualIB}}$ ,  $C_{yy'}^{\text{dualIB}}$  (*theorem 4*) which allows us to claim that they obey the same rules as the  $C$  matrices of the IB.

Similarly to the IB in this calculation we ignore second order contributions which arise from the normalization terms. Considering a variation in  $\hat{x}$  we get:

$$\begin{aligned}
\delta \log p_\beta(x | \hat{x}) &= \beta \sum_y p_\beta(y | \hat{x}) \left( \log \frac{p(y | x)}{p_\beta(y | \hat{x})} - 1 \right) \delta \log p_\beta(y | \hat{x}) \\
&= \beta \sum_y p_\beta(y | \hat{x}) \left[ \log p(y | x) - \sum_{\tilde{x}} p_\beta(\tilde{x} | \hat{x}) \log p(y | \tilde{x}) \right] \delta \log p_\beta(y | \hat{x}) \\
&\quad + \beta \sum_y \log Z_{\mathbf{y}|\hat{\mathbf{x}}}(\hat{x}; \beta) \frac{\partial p_\beta(y | \hat{x})}{\partial \hat{x}} \\
&= \beta \sum_{y, \tilde{x}} p_\beta(y | \hat{x}) p_\beta(\tilde{x} | \hat{x}) \log \frac{p(y | x)}{p(y | \tilde{x})} \delta \log p_\beta(y | \hat{x}), \tag{18}
\end{aligned}$$

$$\begin{aligned}
\delta \log p_\beta(y | \hat{x}) &= - \frac{1}{Z_{\mathbf{y}|\hat{\mathbf{x}}}(\hat{x}; \beta)} \frac{\partial Z_{\mathbf{y}|\hat{\mathbf{x}}}(\hat{x}; \beta)}{\partial \hat{x}} + \sum_x p_\beta(x | \hat{x}) \log p(y | x) \delta \log p_\beta(x | \hat{x}) \\
&= - \sum_{\tilde{y}} p_\beta(\tilde{y} | \hat{x}) \sum_x p_\beta(x | \hat{x}) \log p(\tilde{y} | x) \delta \log p_\beta(x | \hat{x}) \\
&\quad + \sum_x p_\beta(x | \hat{x}) \log p(y | x) \delta \log p_\beta(x | \hat{x}) \\
&= \sum_{x, \tilde{y}} p_\beta(x | \hat{x}) p_\beta(\tilde{y} | \hat{x}) \log \frac{p(y | x)}{p(\tilde{y} | x)} \delta \log p_\beta(x | \hat{x}). \tag{19}
\end{aligned}$$

Substituting (19) into (18) and vice versa one obtains:

$$\begin{aligned}
\delta \log p_\beta(x | \hat{x}) &= \beta \sum_{x', y, \tilde{y}, \tilde{x}} p_\beta(y | \hat{x}) p_\beta(\tilde{x} | \hat{x}) \log \frac{p(y | x)}{p(y | \tilde{x})} \\
&\quad \cdot p_\beta(x' | \hat{x}) p_\beta(\tilde{y} | \hat{x}) \log \frac{p(y | x')}{p(\tilde{y} | x')} \delta \log p_\beta(x' | \hat{x}) \\
\delta \log p_\beta(y | \hat{x}) &= \beta \sum_{x, y', \tilde{x}, \tilde{y}} p_\beta(x | \hat{x}) p_\beta(\tilde{y} | \hat{x}) \log \frac{p(y | x)}{p(\tilde{y} | x)} \\
&\quad \cdot p_\beta(y' | \hat{x}) p_\beta(\tilde{x} | \hat{x}) \log \frac{p(y' | x)}{p(y' | \tilde{x})} \delta \log p_\beta(y' | \hat{x}).
\end{aligned}$$

We now define the  $C^{\text{dualIB}}$  matrices as follows:

$$\begin{aligned}
C_{xx'}^{\text{dualIB}}(\hat{x}; \beta) &= \sum_{y, \tilde{y}, \tilde{x}} p_\beta(y | \hat{x}) p_\beta(\tilde{x} | \hat{x}) \log \frac{p(y | x)}{p(y | \tilde{x})} \cdot p_\beta(x' | \hat{x}) p_\beta(\tilde{y} | \hat{x}) \log \frac{p(y | x')}{p(\tilde{y} | x')} \\
C_{yy'}^{\text{dualIB}}(\hat{x}; \beta) &= \sum_{x, \tilde{x}, \tilde{y}} p_\beta(x | \hat{x}) p_\beta(\tilde{y} | \hat{x}) \log \frac{p(y | x)}{p(\tilde{y} | x)} \cdot p_\beta(y' | \hat{x}) p_\beta(\tilde{x} | \hat{x}) \log \frac{p(y' | x)}{p(y' | \tilde{x})}.
\end{aligned}$$

Using the above definition we have an equivalence to the IB stability analysis in the form of:

$$\left[ I - \beta C_{xx'}^{\text{dualIB}}(\hat{x}, \beta) \right] \delta \log p_\beta(x' | \hat{x}) = 0, \quad \left[ I - \beta C_{yy'}^{\text{dualIB}}(\hat{x}, \beta) \right] \delta \log p_\beta(y' | \hat{x}) = 0.$$

Note that for the binary case, the matrices may be simplified to:

$$\begin{aligned}
C_{xx'}^{\text{dualIB}}(\hat{x}; \beta) &= \sum_{y, \tilde{x}} p_\beta(y | \hat{x}) p_\beta(\tilde{x} | \hat{x}) \log \frac{p(y | x)}{p(y | \tilde{x})} \cdot p_\beta(x' | \hat{x}) (1 - p_\beta(y | \hat{x})) \log \frac{p(y | x')}{1 - p(y | x')} \\
C_{yy'}^{\text{dualIB}}(\hat{x}; \beta) &= \sum_{x, \tilde{x}} p_\beta(x | \hat{x}) (1 - p_\beta(y | \hat{x})) \log \frac{p(y | x)}{1 - p(y | x)} \cdot p_\beta(y' | \hat{x}) p_\beta(\tilde{x} | \hat{x}) \log \frac{p(y' | x)}{p(y' | \tilde{x})}.
\end{aligned}$$

We turn to show that the  $C^{\text{dualIB}}$  matrices share the same eigenvalues with  $\lambda_1(\hat{x}) = 0$ .

*Proof.* The matrices,  $C_{xx'}^{\text{dualIB}}(\hat{x}; \beta)$ ,  $C_{yy'}^{\text{dualIB}}(\hat{x}; \beta)$ , are given by:

$$C_{xx'}^{\text{dualIB}}(\hat{x}; \beta) = A_{xy}(\hat{x}; \beta)B_{yx'}(\hat{x}; \beta), \quad C_{yy'}^{\text{dualIB}}(\hat{x}; \beta) = B_{yx}(\hat{x}; \beta)A_{xy'}(\hat{x}; \beta),$$

with:

$$A_{xy}(\hat{x}; \beta) = p_\beta(y | \hat{x}) \sum_{\tilde{x}} p_\beta(\tilde{x} | \hat{x}) \log \frac{p(y | x)}{p(y | \tilde{x})}, \quad B_{yx}(\hat{x}; \beta) = p_\beta(x | \hat{x}) \sum_{\tilde{y}} p_\beta(\tilde{y} | \hat{x}) \log \frac{p(y | x)}{p(\tilde{y} | x)}.$$

Given that the matrices are obtained by the multiplication of the same matrices, it follows that they have the same eigenvalues  $\{\lambda_i(\hat{x}; \beta)\}$ .

To prove that  $\lambda_1(\hat{x}; \beta) = 0$  we show that  $\det(C_{yy'}^{\text{dualIB}}) = 0$ . We present the exact calculation for a binary label  $y \in \{y_0, y_1\}$  (the argument for general  $y$  follows by encoding the label as a sequence of bits and discussing the first bit only, as a binary case):

$$\begin{aligned} \det(C_{yy'}^{\text{dualIB}}(\hat{x}; \beta)) &= \sum_{x, \tilde{x}} p_\beta(x | \hat{x}) p_\beta(y_1 | \hat{x}) \log \frac{p(y_0 | x)}{p(y_1 | x)} \cdot p_\beta(y_0 | \hat{x}) p_\beta(\tilde{x} | \hat{x}) \log \frac{p(y_0 | x)}{p(y_0 | \tilde{x})} \\ &\quad \cdot \sum_{x', \tilde{x}'} p_\beta(x' | \hat{x}) p_\beta(y_0 | \hat{x}) \log \frac{p(y_1 | x')}{p(y_0 | x')} \cdot p_\beta(y_1 | \hat{x}) p_\beta(\tilde{x}' | \hat{x}) \log \frac{p(y_1 | x')}{p(y_1 | \tilde{x}')} \\ &\quad - \sum_{x, \tilde{x}} p_\beta(x | \hat{x}) p_\beta(y_0 | \hat{x}) \log \frac{p(y_1 | x)}{p(y_0 | x)} \cdot p_\beta(y_0 | \hat{x}) p_\beta(\tilde{x} | \hat{x}) \log \frac{p(y_0 | x)}{p(y_0 | \tilde{x})} \\ &\quad \cdot \sum_{x', \tilde{x}'} p_\beta(x' | \hat{x}) p_\beta(y_1 | \hat{x}) \log \frac{p(y_0 | x')}{p(y_1 | x')} \cdot p_\beta(y_1 | \hat{x}) p_\beta(\tilde{x}' | \hat{x}) \log \frac{p(y_1 | x')}{p(y_1 | \tilde{x}')} \\ &= \sum_{x, x', \tilde{x}, \tilde{x}'} p_\beta(x | \hat{x}) p_\beta(x' | \hat{x}) p_\beta^2(y_0 | \hat{x}) p_\beta^2(y_1 | \hat{x}) p_\beta(\tilde{x} | \hat{x}) \log \frac{p(y_0 | x)}{p(y_0 | \tilde{x})} p_\beta(\tilde{x}' | \hat{x}) \log \frac{p(y_1 | x')}{p(y_1 | \tilde{x}')} \\ &\quad \cdot \left[ \log \frac{p(y_0 | x)}{p(y_1 | x)} \log \frac{p(y_1 | x')}{p(y_0 | x')} - \log \frac{p(y_0 | x)}{p(y_1 | x)} \log \frac{p(y_1 | x')}{p(y_0 | x')} \right] = 0. \end{aligned}$$

Given that the determinant is 0 implies that  $\lambda_1(\hat{x}) = 0$ . □

For a binary problem we can describe the non-zero eigenvalue using  $\lambda_2(\hat{x}) = \text{Tr}(C_{yy'}^{\text{dualIB}}(\hat{x}; \beta))$ . That is:

$$\begin{aligned} \lambda_2(\hat{x}) &= \sum_{x, \tilde{x}} p_\beta(x | \hat{x}) p_\beta(y_1 | \hat{x}) \log \frac{p(y_0 | x)}{p(y_1 | x)} \cdot p_\beta(y_0 | \hat{x}) p_\beta(\tilde{x} | \hat{x}) \log \frac{p(y_0 | x)}{p(y_0 | \tilde{x})} \\ &\quad + \sum_{x, \tilde{x}} p_\beta(x | \hat{x}) p_\beta(y_0 | \hat{x}) \log \frac{p(y_1 | x)}{p(y_0 | x)} \cdot p_\beta(y_1 | \hat{x}) p_\beta(\tilde{x} | \hat{x}) \log \frac{p(y_1 | x)}{p(y_1 | \tilde{x})} \\ &= p_\beta(y_1 | \hat{x}) p_\beta(y_0 | \hat{x}) \sum_{x, \tilde{x}} p_\beta(x | \hat{x}) p_\beta(\tilde{x} | \hat{x}) \log \frac{p(y_0 | x)}{p(y_1 | x)} \left[ \log \frac{p(y_0 | x)}{p(y_0 | \tilde{x})} - \log \frac{p(y_1 | x)}{p(y_1 | \tilde{x})} \right]. \end{aligned}$$

### D.1 Definition of the sample problem

We consider a problem for a binary label  $Y$  and 5 possible inputs  $X$  uniformly distributed, i.e.  $\forall x \in \mathcal{X}, p(x) = 1/5$  and the conditional distribution,  $p(y | x)$ , given by:

	$x = 0$	$x = 1$	$x = 2$	$x = 3$	$x = 4$
$y = 0$	0.12	0.23	0.4	0.6	0.76
$y = 1$	0.88	0.77	0.6	0.4	0.24

## E Information plane analysis

We rely on known results for the rate-distortion problem and the information plane:

**Lemma 7.**  $I(x; \hat{X})$  is a non-increasing convex function of the distortion  $\mathbb{E}_{p_\beta(x, \hat{x})}[d(x, \hat{x})]$  with a slope of  $-\beta$ .

We emphasize that this is a general result of rate-distortion thus holds for the dualIB as well.

**Lemma 8.** For a fixed encoder  $p_\beta(\hat{x} | x)$  and the Bayes optimal decoder  $p_\beta(y | \hat{x})$ :

$$\mathbb{E}_{p_\beta(x, \hat{x})}[d_{\text{IB}}(x, \hat{x})] = I(X; Y) - I(\hat{X}; Y).$$

Thus, the information curve,  $I_y$  vs.  $I_x$ , is a non-decreasing concave function with a positive slope,  $\beta^{-1}$ . The concavity implies that  $\beta$  increases along the curve.

[13, 18].

### E.1 Proof of Lemma 3

In the following section we provide a proof to lemma 3, for the IB and dualIB problems.

*Proof.* We want to analyze the behavior of  $I_x(\beta)$ ,  $I_y(\beta)$ , that is the change in each term as a function of the corresponding  $\beta$ . From lemma 8, the concavity of the information curve, we can deduce that both are non-decreasing functions of  $\beta$ . As the two  $\beta$  derivatives are proportional it's enough to discuss the first one.

Next, we focus on their behavior between two critical points. That is, where the cardinality of  $\hat{X}$  is fixed (clusters are "static"). For "static" clusters, the  $\beta$  derivative of  $I_x$ , along the optimal line is given by:

$$\begin{aligned} \frac{\partial I(X; \hat{X})}{\partial \beta} &= -\frac{\partial}{\partial \beta} \left[ \sum_{x, \hat{x}} p_\beta(x, \hat{x}) (\log Z_{\hat{x}|x}(x; \beta) + \beta d(x, \hat{x})) \right] \\ &= -\beta \left\langle d(x, \hat{x}) \frac{\partial \log p_\beta(\hat{x} | x)}{\partial \beta} \right\rangle_{p_\beta(x, \hat{x})} \\ &\approx \beta \left\langle d(x, \hat{x}) \left[ \frac{\partial \log Z_{\hat{x}|x}(x; \beta)}{\partial \beta} + d(x, \hat{x}) \right] \right\rangle_{p_\beta(x, \hat{x})} \\ &\approx \beta \left\langle \underbrace{\langle d^2(x, \hat{x}) \rangle_{p_\beta(\hat{x}|x)}}_{\text{Var}(d(x))} - \underbrace{\langle d(x, \hat{x}) \rangle_{p_\beta(\hat{x}|x)}^2}_{p(x)} \right\rangle_{p(x)}. \end{aligned}$$

This first of all reassures that the function is non-decreasing as  $\text{Var}(d(x)) \geq 0$ .

The piece-wise concavity follows from the fact that when the number of clusters is fixed (between the critical points) - increasing  $\beta$  decreases the clusters conditional entropy  $H(\hat{X} | x)$ , as the encoder becomes more deterministic. The mutual information is bounded by  $H(\hat{X})$  and it's  $\beta$  derivative decreases. Further, between the critical points there are no sign changes in the second  $\beta$  derivative.  $\square$

### E.2 Proof of Theorem 4

*Proof.* The proof follows from lemma 3 together with the critical points analysis above, and is only sketched here. As the encoder and decoder at the critical points,  $\beta_c^{\text{IB}}$  and  $\beta_c^{\text{dualIB}}$ , have different left and right derivatives, they form cusps in the curves of the mutual information ( $I_x$  and  $I_y$ ) as functions of  $\beta$ . These cusps can only be consistent with the optimality of the IB curves (implying that sub-optimal curves lie below it; i.e, the IB slope is steeper) if  $\beta_c^{\text{dualIB}} < \beta_c^{\text{IB}}$  (this is true for any sub-optimal distortion), otherwise the curves intersect.

Moreover, at the dualIB critical points, the distance between the curves is minimized due to the strict concavity of the functions segments between the critical points. As the critical points imply discontinuity in the derivative, this results in a "jump" in the information values. Therefore, at any  $\beta_c^{\text{dualIB}}$  the distance between the curves has a (local) minimum. This is depicted in Figure 4 (in the main text), comparing  $I_x(\beta)$  and  $I_y(\beta)$  and their differences for the two algorithms.



The two curves approach each other for large  $\beta$  since the two distortion functions become close in the low distortion limit (as long as  $p(y | x)$  is bounded away from 0).  $\square$

## F Derivation of the dualExpIB

We provide elaborate derivations to *theorem 9*; that is, we obtain the dualIB optimal encoder-decoder under the exponential assumption over the data. We use the notations defined in §*The Exponential Family dualIB*.

- The *decoder*. Substituting the exponential assumption into the dualIB log-decoder yields:

$$\begin{aligned} \log p_\beta(y | \hat{x}) &= \sum_x p_\beta(x | \hat{x}) \log p(y | x) - \log Z_{\mathbf{y}|\hat{\mathbf{x}}}(\hat{x}; \beta) \\ &= - \sum_x \sum_{r=0}^d p_\beta(x | \hat{x}) \lambda^r(y) A_r(x) - \log Z_{\mathbf{y}|\hat{\mathbf{x}}}(\hat{x}; \beta) \\ &= - \sum_{r=1}^d \lambda^r(y) A_{r,\beta}(\hat{x}) - \mathbb{E}_{p_\beta(x|\hat{x})} [\lambda_{\mathbf{x}}^0] - \log Z_{\mathbf{y}|\hat{\mathbf{x}}}(\hat{x}; \beta). \end{aligned}$$

Taking a closer look at the normalization term:

$$\begin{aligned} Z_{\mathbf{y}|\hat{\mathbf{x}}}(\hat{x}; \beta) &= \sum_y e^{\sum_x p_\beta(x|\hat{x}) \log p(y|x)} = e^{-\mathbb{E}_{p_\beta(x|\hat{x})} [\lambda_{\mathbf{x}}^0]} \sum_y e^{-\sum_{r=1}^d \lambda^r(y) A_{r,\beta}(\hat{x})} \\ \log Z_{\mathbf{y}|\hat{\mathbf{x}}}(\hat{x}; \beta) &= -\mathbb{E}_{p_\beta(x|\hat{x})} [\lambda_{\mathbf{x}}^0] + \log \left( \sum_y e^{-\sum_{r=1}^d \lambda^r(y) A_{r,\beta}(\hat{x})} \right). \end{aligned}$$

From which it follows that  $\lambda_\beta^0(\hat{x})$  is given by:

$$\lambda_\beta^0(\hat{x}) = \log \left( \sum_y e^{-\sum_{r=1}^d \lambda^r(y) A_{r,\beta}(\hat{x})} \right),$$

and we can conclude that the dualExpIB decoder takes the form:

$$\log p_\beta(y | \hat{x}) = - \sum_{r=1}^d \lambda^r(y) A_{r,\beta}(\hat{x}) - \lambda_\beta^0(\hat{x}).$$

- The *encoder*.  
The core of the encoder is the dual distortion function which may now be written as:

$$\begin{aligned} d_{\text{dualIB}}(x, \hat{x}) &= \sum_y p_\beta(y | \hat{x}) \log \frac{p_\beta(y | \hat{x})}{p(y | x)} \\ &= \sum_y p_\beta(y | \hat{x}) \left[ (\lambda_{\mathbf{x}}^0 - \lambda_\beta^0(\hat{x})) + \sum_{r=1}^d \lambda^r(y) (A_r(x) - A_{r,\beta}(\hat{x})) \right] \\ &= \lambda_{\mathbf{x}}^0 - \lambda_\beta^0(\hat{x}) + \sum_{r=1}^d \lambda_\beta^r(\hat{x}) (A_r(x) - A_{r,\beta}(\hat{x})), \end{aligned}$$

substituting this into the encoder's definition we obtain:

$$\begin{aligned} p_\beta(\hat{x} | x) &= \frac{p_\beta(\hat{x})}{Z_{\hat{\mathbf{x}}|\mathbf{x}}(x; \beta)} e^{-\beta[\lambda_{\mathbf{x}}^0 - \lambda_\beta^0(\hat{x}) + \sum_{r=1}^d \lambda_\beta^r(\hat{x}) (A_r(x) - A_{r,\beta}(\hat{x}))]} \\ &= \frac{p_\beta(\hat{x}) e^{\beta \lambda_\beta^0(\hat{x})}}{Z_{\hat{\mathbf{x}}|\mathbf{x}}(x; \beta)} e^{-\beta \sum_{r=1}^d \lambda_\beta^r(\hat{x}) (A_r(x) - A_{r,\beta}(\hat{x}))}. \end{aligned}$$

We can further write down the information quantities under these assumptions:

$$\begin{aligned}
I(X; \hat{X}) &= \sum_{x, \hat{x}} p_\beta(x, \hat{x}) \log \frac{p_\beta(x | \hat{x})}{p(x)} \\
&= H(X) - \beta \sum_{r=1}^d \sum_{\hat{x}} p_\beta(\hat{x}) \lambda_\beta^r(\hat{x}) \left[ \sum_x p_\beta(x | \hat{x}) A_r(x) - A_{r, \beta}(\hat{x}) \right] + \beta \mathbb{E}_{p_\beta(\hat{x})} [\lambda_\beta^0(\hat{x})] - \mathbb{E}_{p(x)} [\log Z_{\hat{x}|\mathbf{x}}(x; \beta)] \\
&= H(X) + \beta \mathbb{E}_{p_\beta(\hat{x})} [\lambda_\beta^0(\hat{x})] - \mathbb{E}_{p(x)} [\log Z_{\hat{x}|\mathbf{x}}(x; \beta)] \\
I(Y; \hat{X}) &= \sum_{y, \hat{x}} p_\beta(y, \hat{x}) \log \frac{p_\beta(y | \hat{x})}{p(y)} \\
&= H(Y) - \sum_{r=1}^d \sum_{\hat{x}} p_\beta(\hat{x}) \sum_y p_\beta(y | \hat{x}) \lambda^r(y) A_{r, \beta}(\hat{x}) - \mathbb{E}_{p_\beta(\hat{x})} [\lambda_\beta^0(\hat{x})] \\
&= H(Y) - \mathbb{E}_{p_\beta(\hat{x})} \left[ \sum_{r=1}^d \lambda_\beta^r(\hat{x}) A_{r, \beta}(\hat{x}) + \lambda_\beta^0(\hat{x}) \right]
\end{aligned}$$

## G Optimizing the error exponent

We start by to expressing the Chernoff information for the binary hypothesis testing problem using  $p(y | x)$ :

$$\begin{aligned}
C(p_0, p_1) &= \min_{\lambda \in [0, 1]} \log \left( \sum_x p(x | y_0)^{q_\lambda(y_0)} p(x | y_1)^{q_\lambda(y_1)} \right) \\
&= \min_{\lambda \in [0, 1]} \log \left( \sum_x p(y = 0 | x)^\lambda p(x)^\lambda p(y = 0)^{-\lambda} p(y = 1 | x)^{1-\lambda} p(x)^{1-\lambda} p(y = 1)^{\lambda-1} \right) \\
&= \min_{\lambda \in [0, 1]} \log \left( \sum_x p(x) p(y = 0 | x)^\lambda p(y = 1 | x)^{1-\lambda} \right) - \log \left( p(y = 0)^\lambda p(y = 1)^{1-\lambda} \right) \\
&= \min_{q_\lambda(y)} \log \left( \sum_x e^{q_\lambda(y_0) \log p(x|y_0) + q_\lambda(y_1) \log p(x|y_1)} \right) \\
&= \min_{q_\lambda(y)} \log \left( \sum_x e^{-D[q_\lambda(y) \| p(y|x)] + D[q_\lambda(y) \| p(y)] + \log p(x)} \right) \\
&= \min_{q_\lambda(y)} \log \left( e^{D[q_\lambda(y) \| p(y)]} \sum_x e^{-D[q_\lambda(y) \| p(y|x)] + \log p(x)} \right) \\
&= \min_{q_\lambda(y)} \left\{ \log \left( \sum_x p(x) e^{-D[q_\lambda(y) \| p(y|x)]} \right) + D[q_\lambda(y) \| p(y)] \right\},
\end{aligned}$$

where  $q_\lambda(y_0) = \lambda, q_\lambda(y_1) = 1 - \lambda$ . Now, if we consider the mapping,  $q_\lambda(y) = p_\beta(y | \hat{x})$  we can write the above as:

$$C(p_0, p_1) = \min_{p_\beta(y|\hat{x})} \left\{ \log \left( \sum_x p(x) e^{-D[p_\beta(y|\hat{x}) \| p(y|x)]} \right) + D[p_\beta(y | \hat{x}) \| p(y)] \right\}.$$

The above term in minimization is proportional to log-partition function of  $p_\beta(x | \hat{x})$ , namely we get the mapping  $p_\beta(x | \hat{x}) = p_\lambda$ . Next we shall generalize the setting to the  $M$ -hypothesis testing problem. Having that solving for the Chernoff information is notoriously difficult we consider an upper bound to it, taking the expectation over the classes. Instead of choosing  $p_{\lambda^*}$  as the maximal value of the minimum  $\{D[p_{\lambda^*} \| p_0], D[p_{\lambda^*} \| p_1]\}$  we consider it w.r.t the full set  $\{D[p_{\lambda^*} \| p_i]\}_{i=1}^M$ . Using the above mapping we must take the expectation also over the representation variable  $\hat{x}$ . Thus

we get the expression:

$$D^*(\beta) = \min_{p_\beta(y|\hat{x}), p_\beta(\hat{x}|x)} \mathbb{E}_{p_\beta(y, \hat{x})} [D[p_\beta(x | \hat{x}) | p(x | y)]].$$

From the definition of  $D^*(\beta)$  we obtain the desired bound of the dualIB:

$$\begin{aligned} D^*(\beta) &= \min_{p_\beta(y|\hat{x}), p_\beta(\hat{x}|x)} \mathbb{E}_{p_\beta(y, \hat{x})} [D[p_\beta(x | \hat{x}) | p(x | y)]] \\ &= \min_{p_\beta(y|\hat{x}), p_\beta(\hat{x}|x)} \sum_{x, y, \hat{x}} p_\beta(y | \hat{x}) p_\beta(\hat{x} | x) [D[p_\beta(x | \hat{x}) | p(x | y)]] \\ &= \min_{p_\beta(y|\hat{x}), p_\beta(\hat{x}|x)} \sum_{x, y, \hat{x}} p_\beta(y | \hat{x}) p_\beta(\hat{x} | x) p_\beta(x | \hat{x}) \left\{ \log \frac{p_\beta(y | \hat{x})}{p(y | x)} + \log \frac{p_\beta(x | \hat{x})}{p_\beta(y | \hat{x})} + \log \frac{p(y)}{p(x)} \right\} \\ &= \min_{p_\beta(y|\hat{x}), p_\beta(\hat{x}|x)} \left\{ I(X; \hat{X}) + \mathbb{E}_{p_\beta(x, \hat{x})} [D[p_\beta(y | \hat{x}) | p(y | x)]] + H(Y | \hat{X}) + \mathbb{E}_{p_\beta(y)} [\log p(y)] \right\} \\ &\leq \min_{p_\beta(y|\hat{x}), p_\beta(\hat{x}|x)} \left\{ I(X; \hat{X}) + \mathbb{E}_{p_\beta(x, \hat{x})} [D[p_\beta(y | \hat{x}) | p(y | x)]] \right\} \\ &\leq \mathcal{F}^*[p(\hat{x} | x); p(y | \hat{x})]. \end{aligned}$$

### G.1 Error exponent optimization example

To demonstrate the above properties we consider a classification problem with  $M = 8$  classes, each class characterized by  $p_i = p(x | y_i)$ . The *training* is performed according to the above algorithms to obtain the IB (dualIB) encoder and decoder. For the prediction, given a new sample  $x^{(n)}$  *i.i.d.*  $p(x | y)$  defining an empirical distribution  $\hat{p}(x)$  the prediction is done by first evaluating  $\hat{p}_\beta(\hat{x}) = \sum_x p_\beta(\hat{x} | x) \hat{p}(x)$ . Next, using the (representation) optimal decision rule, we obtain the prediction:

$$\hat{H}_\beta = \arg \min_i D[\hat{p}_\beta(\hat{x}) | p_\beta(\hat{x} | y_i)],$$

and we report  $p_{err}^{(n)}$ , the probability of miss-classification. This represents the most general classification task; the distributions  $p_i$  represent the empirical distributions over a training data-set and then testing is performed relative to a test set. Looking at the results, Figure A1, it is evident that indeed the dualIB improves the prediction error (at  $\log_2(\beta) = 6$  the algorithms performance is identical due to the similarity of the algorithms behavior as  $\beta$  increases).

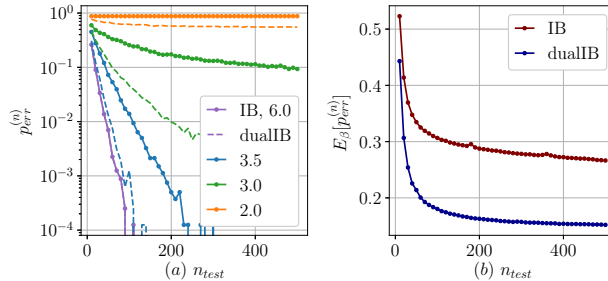


Figure A1: The probability of error,  $p_{err}^{(n)}$ , as a function of test sample size,  $n_{test}$ . (a) The exponential decay of error for representative  $\beta$  values ( $\log_2(\beta)$  reported in the legend). For a given  $\beta$  the IB performance is plotted in solid line and the dualIB in dashed (for  $\log_2(\beta) = 6$  the lines overlap). (b) The expectation of the error over all  $\beta$ 's ( $\log_2 \beta \in [1, 6]$ ).

## H The variational dualIB

### H.1 Derivation of the VdualIB objective

Just as [26] did, we can variationally upper bound the information of the input with the representation variable using:

$$I(\hat{X}; X | Y) = \mathbb{E}_{p(x,y)p(\hat{x}|x)} \left[ \log \frac{p(\hat{x} | x, y)}{p(\hat{x} | y)} \right] \leq \mathbb{E}_{\tilde{p}(y|x)p(x)p(\hat{x}|x)} \left[ \log \frac{p(\hat{x} | x)}{q(\hat{x} | y)} \right]$$

where  $q(\hat{x} | y)$  is a variational class conditional marginal. In contradiction to the CEB, in order to bound the dualIB distortion, we replace the bound on  $I(\hat{X}; Y)$  with a bound over the expected dualIB distortion. Here, given the assumption of a noise model  $\tilde{p}(y | x)$  which we evaluate the expected distortion with respect to it:

$$\mathbb{E}_{p(x,\hat{x})}[d_{\text{dualIB}}(x, \hat{x})] = \mathbb{E}_{p(y|\hat{x})p(\hat{x}|x)p(x)} \left[ \log \frac{p(y | \hat{x})}{\tilde{p}(y | x)} \right]$$

Combining the above together gives the variational upper bound to the dualIB as the following objective:

$$I(X; \hat{X}) + \beta \mathbb{E}_{p(x,\hat{x})}[d_{\text{dualIB}}(x, \hat{x})] \leq \mathbb{E}_{\tilde{p}(y|x)p(\hat{x}|x)p(x)} \left[ \log \frac{p(\hat{x} | x)}{q(\hat{x} | y)} \right] + \beta \mathbb{E}_{p(y|\hat{x})p(\hat{x}|x)p(x)} \left[ \log \frac{p(y | \hat{x})}{\tilde{p}(y | x)} \right]$$

### H.2 Experimental setup

For both CIFAR10 and FashionMNIST We trained a set of 30 28 – 10 Wide ResNet models in a range of values of  $\beta$  ( $-5 \leq \log \beta \leq 5$ ). The training was done using Adam [35] at a base learning rate of  $10^{-4}$ . We lowered the learning rate two times by a factor of 0.3 each time. Additionally, following [26], we use a jump-start method for  $\beta < 100$ . We start the training with  $\beta = 100$ , anneal down to the target  $\beta$  over 1000 steps. The training includes data augmentation with horizontal flip and width height shifts. Note, that we exclude from the analysis runs that didn't succeed to learn at all (for which the results look as random points).

### H.3 The variational information plane

Note that, for the information plane analysis, there were several runs that failed to achieved more than random accuracy. In such cases, we remove them. The confusion matrix used for the FashionMNIST data-set is:

$$\begin{pmatrix} 0.828 & 0.013 & 0.012 & 0.011 & 0.018 & 0. & 0.002 & 0.004 & 0.085 & 0.027 \\ 0.01 & 0.91 & 0. & 0.005 & 0.001 & 0.001 & 0. & 0.001 & 0.011 & 0.061 \\ 0.047 & 0.001 & 0.708 & 0.064 & 0.088 & 0.014 & 0.063 & 0.004 & 0.008 & 0.003 \\ 0.003 & 0.004 & 0.016 & 0.768 & 0.033 & 0.093 & 0.05 & 0.019 & 0.004 & 0.01 \\ 0.01 & 0. & 0.039 & 0.043 & 0.788 & 0.012 & 0.057 & 0.043 & 0.006 & 0.002 \\ 0.002 & 0. & 0.01 & 0.137 & 0.029 & 0.777 & 0.008 & 0.033 & 0. & 0.004 \\ 0.007 & 0.002 & 0.01 & 0.054 & 0.029 & 0.007 & 0.888 & 0.001 & 0.001 & 0.001 \\ 0.024 & 0.002 & 0.014 & 0.039 & 0.076 & 0.017 & 0.004 & 0.818 & 0.002 & 0.004 \\ 0.027 & 0.013 & 0. & 0.007 & 0.003 & 0. & 0.003 & 0. & 0.933 & 0.014. \\ 0.019 & 0.064 & 0.001 & 0.007 & 0.002 & 0.001 & 0.001 & 0. & 0.018 & 0.887 \end{pmatrix}$$

### H.4 The VdualIB noise models

As described in the main text we consider two additional noise models; (i) An analytic Gaussian integration of the log-loss around the one-hot labels (AnGVdualIB) (ii) Using predictions of another trained model as the induced distribution (PrdTrVdualIB). In this case, we use a deterministic wide ResNet 28 – 10 network that achieved 95.8% accuracy on CIFAR10. In Figure A2 we can see all the different models, 4 noise models for the VdualIB and the VIB). As expected, we can see that analytic Gaussian integration noise model obtains similar results to adding Gaussian noise to the one-hot vector of the true label, while the performance of the noise models that are based on a trained network are similar to the ConfVdualIB.

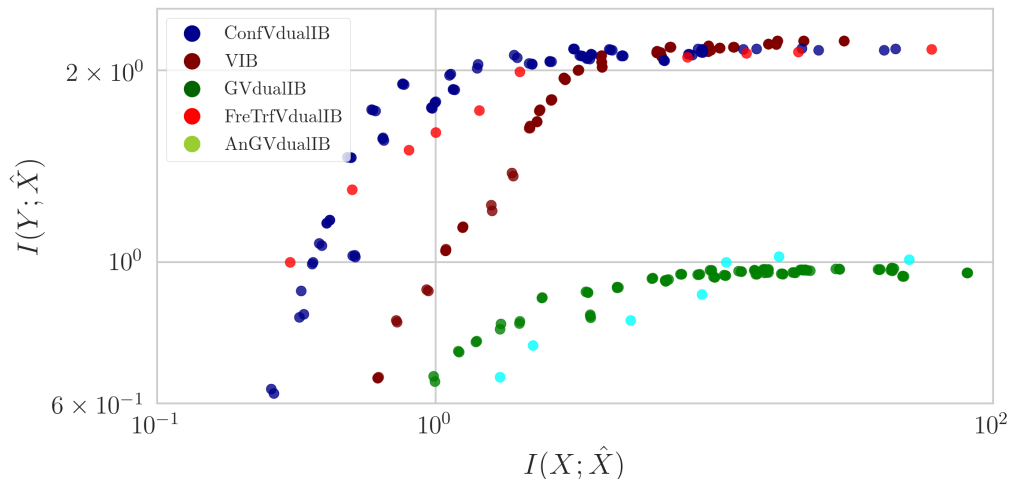


Figure A2: The information plane for the different noise models.

#### H.4.1 Training VIB model with noise

In our analysis, we train a VIB model with the same noise model as the VdualIB. Namely, instead of training with a deterministic label (one-hot vector of zeros and ones), we use our noise model also for the VIB. As mentioned in the text, this training procedure is closely related to label smoothing. In Figure A3, we present the loss function of the VIB on CIFAR10 with and without the noise models along the training process for 3 different values of  $\beta$ . For a small  $\beta$  (left) both regimes under-fit the data as expected. However, when we enlarge  $\beta$ , we can see that the labels' noise makes the training more stable and for a high value of  $\beta$  (right) training without noise over-fits the data and the loss increases.

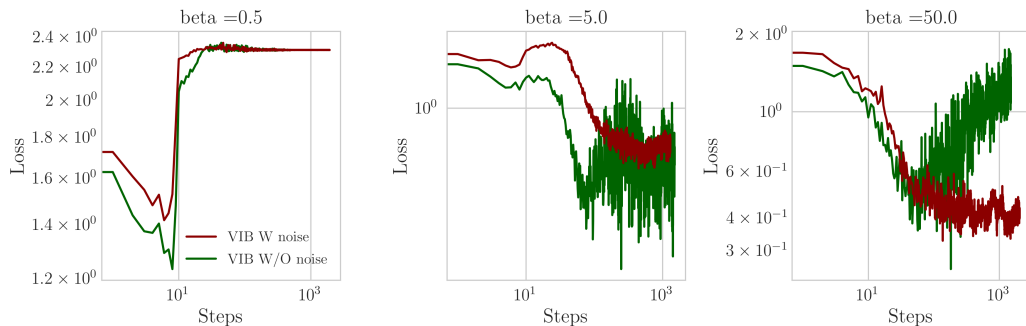


Figure A3: The influence of a noise model on the VIB performance. Loss as function of the update steps for different values of  $\beta$ ,  $\beta = 0.5, 5.0, 50.0$  from left to right.

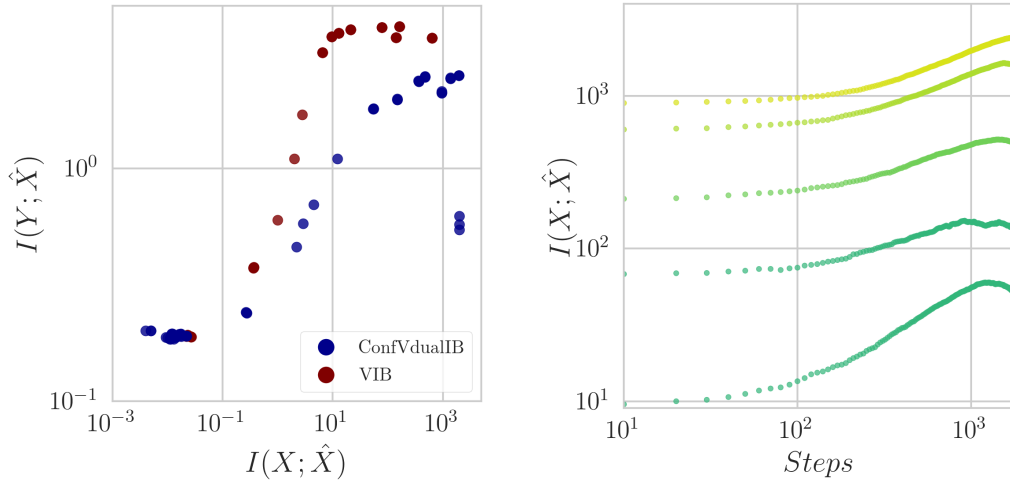
The confusion matrix for the CIFAR10 data set is:

$$\begin{pmatrix} 0.878 & 0. & 0.017 & 0.013 & 0.002 & 0.001 & 0.082 & 0. & 0.007 & 0. \\ 0. & 0.984 & 0.002 & 0.009 & 0.001 & 0. & 0.003 & 0. & 0. & 0. \\ 0.013 & 0.001 & 0.896 & 0.009 & 0.038 & 0. & 0.043 & 0. & 0. & 0. \\ [0.022 & 0.004 & 0.011 & 0.913 & 0.023 & 0. & 0.027 & 0. & 0.001 & 0. \\ 0. & 0. & 0.072 & 0.022 & 0.85 & 0. & 0.058 & 0. & 0. & 0. \\ 0. & 0. & 0. & 0. & 0. & 0.982 & 0. & 0.011 & 0. & 0.007 \\ 0.099 & 0.001 & 0.049 & 0.021 & 0.055 & 0. & 0.768 & 0. & 0.005 & 0. \\ 0. & 0. & 0. & 0. & 0. & 0.006 & 0. & 0.976 & 0. & 0.019 \\ 0.004 & 0.001 & 0.001 & 0.001 & 0.004 & 0.002 & 0.003 & 0.001 & 0.98 & 0.001 \\ 0. & 0. & 0. & 0. & 0. & 0.004 & 0. & 0.02 & 0.001 & 0.974 \end{pmatrix}$$

### H.5 CIFAR100 results

As mentioned in the text, we trained VdualIB networks also on CIFAR100. For this, we used the same 28 – 10 Wide ResNet with a confusion matrix as our noise model. The confusion matrix was calculated based on the predictions of a deterministic network. The deterministic network achieved 80.2% accuracy on CIFAR100. In A4a, we can see the information plane for both VdualIB and the VIB models. As we can see, both models are monotonic with  $I(X; \hat{X})$ , however the VIB’s performance is better. The VIB achieves higher values of information with the labels along with more compressed representation at any given level of predication. Although a broader analysis is required, and possible further parameter tuning of the architecture, we hypothesize that the caveat is in the noise model used for the VdualIB. Using a noise model which is based on a network that achieves almost 20% error might be insufficient in this case. It might be that “errors” in the noise model becomes similar to random errors, similar to the Gaussian case, and hence depicting similar learning performance to the GVdualIB case.

When we look at the information with the input as a function of time ,Figure A4b, we see that similar to the FasionMNIST and CIFAR10 results, the information saturates for small values of  $\beta$ , but over-fits for higher values of it.



(a) The information plane

(b)  $I(X; \hat{X})$  vs. update steps for different  $\beta$ ’s

Figure A4: Experiments over CIFAR100. (a) The information plane of the ConfVdualIB and VIB for a range of  $\beta$  values at the final training step. (b) The evolution of the the ConfVdualIB’s  $I(X; \hat{X})$  along the optimization update steps.